JOURNAL OF Materials CHEMISTRY

Photoinduced processes in fullerenopyrrolidine and fullerenopyrazoline derivatives substituted with an oligophenylenevinylene moiety†

Nicola Armaroli,*[a] Gianluca Accorsi,[a] Jean-Paul Gisselbrecht,[b] Maurice Gross,*[b] Victor Krasnikov,[c] Dimitris Tsamouras,[c] Georges Hadziioannou,*[c]‡ María J. Gómez-Escalonilla,[d] Fernando Langa,*[d] Jean-François Eckert[e] and Jean-François Nierengarten*[e]

[a]*Istituto per la Sintesi Organica e la Fotoreattività, Laboratorio di Fotochimica, Consiglio Nazionale della Ricerche, via Gobetti 101, 40129 Bologna, Italy. E-mail: armaroli@frae.bo.cnr.it; Fax: +39-051-6399844*
[b]*Laboratoire d'Electrochimie et de Chimie Physique du Corps Solide, Université Louis Pasteur et CNRS (UMR 7512), 4 rue Blaise Pascal, 67008 Strasbourg, France. E-mail: gross@chimie.u-strasbg.fr*
[c]*Department for Polymer Chemistry and Materials Science Center, University of Groningen, Nijenborgh 4, 9747 AG Groningen, The Netherlands. E-mail: hadzii@chem.rug.nl*
[d]*Facultad de Ciencias del Medio Ambiente, Universidad de Castilla-La Mancha, 45071 Toledo, Spain. E-mail: flanga@amb-to.uclm.es*
[e]*Institut de Physique et Chimie des Matériaux de Strasbourg, Groupe des Matériaux Organiques, Université Louis Pasteur et CNRS (UMR 7504), 23 rue du Loess 67037 Strasbourg, France. E-mail: Jean-Francois.Nierengarten@ipcms.u-strasbg.fr*

Received 2nd January 2002, Accepted 22nd March 2002
First published as an Advance Article on the web 30th April 2002

Fullerene derivatives **A-3PV** and **B-3PV** in which an oligophenylenevinylene trimeric subunit (3PV) is attached to C_{60} through, respectively, a pyrrolidine or a pyrazoline ring have been prepared. The electrochemical and excited-state properties of the multicomponent arrays **A-3PV** and **B-3PV** have been investigated in solution using the related oligophenylenevinylene derivative 3PV, fullerenopyrrolidine **A** and fullerenopyrazoline **B** as reference compounds. In **A-3PV** quantitative OPV → C_{60} photoinduced singlet–singlet energy transfer has been observed. Population of the lowest fullerene singlet excited state is followed by nearly quantitative intersystem crossing to the lowest fullerene triplet excited state in CH_2Cl_2 and toluene, whereas OPV → C_{60} electron transfer is able to compete significantly in the more polar solvent benzonitrile. In the case of **B-3PV**, the excited-state properties are more complex due to the electron donating ability of the pyrazoline ring. As observed for **A-3PV**, quantitative OPV → C_{60} photoinduced singlet–singlet energy transfer occurs in **B-3PV**. However, in this case, the population of the lowest fullerene singlet excited state is followed by an efficient electron transfer from the pyrazoline ring in CH_2Cl_2 and benzonitrile. In **B-3PV**, studies of the dependence of photoinduced processes on solvent polarity, addition of acid, and temperature also reveal that this compound can be considered as a fullerene-based molecular switch, the switchable parameters being the photoinduced processes. Finally, **A-3PV** and **B-3PV** have been tested as active materials in photovoltaic devices and the differences of light to energy conversion efficiencies found for the two compounds have been rationalised on the basis of their photophysical properties.

Introduction

In the light of their particular electronic properties, fullerene derivatives appear to be interesting building blocks for the construction of new photochemical molecular devices.[1–3] Fullerene derivatives covalently bound to a number of donors have been prepared and these systems may exhibit photoinduced intramolecular processes such as electron or energy transfer.[1,2,4–7] Among others, amines are an interesting type of electron donor, since their ability to reduce the carbon sphere upon light irradiation can be controlled by pH and solvent polarity.[8–13] It should also be pointed out that the fullerene sphere is a particularly interesting electron acceptor in artificial photosynthetic models because of its symmetrical shape, its large size, and the properties of its π-electron system.[14] The characteristics of C_{60} successfully compare with those of common acceptors with smaller size such as benzoquinone.[15,16] In fact, accelerated charge separation and decelerated charge recombination have been observed in a fullerene-based acceptor–donor system when compared to the equivalent benzoquinone-based system.[15,16] This has been rationalized by the smaller reorganization energy (λ) of C_{60} compared with those of other acceptors: the smaller reorganization energy of C_{60} positions the photoinduced charge separation rate upward along the normal region of the Marcus parabolic curve, while forcing the charge recombination rate downward in the inverted region.[17] The efficient photogeneration of long lived

†Electronic supplementary information (ESI) available: synthetic procedures and full characterization of all new compounds. See http://www.rsc.org/suppdata/jm/b2/b200432a/

‡*Present address*: Ecole Européenne Chimie Polymères Matériaux (ECPM), Université Louis Pasteur, 25 rue Becquerel, F-67087 Strasbourg Cedex 2, France.

charge-separated states by photoinduced electron transfer is of particular interest for initiating photocatalytic reactions or for solar energy conversion.[1,18]

Following the first preparation of photovoltaic devices from fullerene–oligophenylenevinylene conjugates,[19] a great deal of attention has been devoted to C_{60} fullerene arrays substituted with π-conjugated oligomers such as oligophenylenevinylenes (OPV)[19–23] and related systems[24–27] When compared to photovoltaic devices based on interpenetrating blends of donor (conjugated polymer) and acceptor (C_{60}), chemically linked OPV–fullerene derivatives offer the possibility of obtaining a homogeneous molecular network of molecular p–n junctions. Even if the efficiencies of the molecular photovoltaic systems are still low, it is important to highlight that the behavior of a unique molecule in a photovoltaic cell and the study of its electronic properties allow us to obtain easily structure–activity relationships for a better understanding of the photovoltaic system. In particular, photophysical studies of OPV–C_{60} hybrids in solution have demonstrated that ultrafast OPV → C_{60} singlet–singlet energy transfer competes strongly with the desired electron transfer process, and this can be one of the reasons for their low photovoltaic efficiency.[21]

In this paper, we describe the synthesis and the electrochemistry of a new fullerenopyrazoline molecule (**B**) and of a new OPV–C_{60} molecular array (**A-3PV**). In dichloromethane solution, photoinduced electron transfer (pyrazoline → C_{60}) is detected in the former, whereas in the latter an OPV → C_{60} energy transfer is preferred. A more sophisticated array containing both the pyrazoline and the OPV moiety has been prepared and characterized (**B-3PV**), with the aim of integrating both the energy donor (OPV) and the electron donor (pyrazoline) subunit onto the C_{60} moiety. The photophysical properties of **B**, **A-3PV**, and **B-3PV** have been also studied in toluene (PhMe) and benzonitrile (PhCN) both at room temperature and at 77 K, in order to test the dependence and competition of photoinduced processes by solvent polarity and temperature. Finally, **A-3PV** and **B-3PV** have been tested as active materials in photovoltaic devices and the differences of light to energy conversion efficiencies found for the two compounds rationalised on the basis of their photophysical properties.

Results and discussion

Synthesis

The synthesis of 3PV and **A-3PV** is shown in Scheme 1. Compound **1** was prepared as previously reported.[28] Treatment of **1** with CF_3CO_2H in CH_2Cl_2–H_2O and subsequent $LiAlH_4$ reduction of the resulting aldehyde **2** yielded reference compound 3PV. The functionalization of C_{60} with the OPV group was based on the 1,3-dipolar cycloaddition[29] of the azomethine ylide generated *in situ* from aldehyde **2** and *N*-phenylglycine. The reaction of C_{60} with **2** in the presence of an excess of *N*-phenylglycine in refluxing toluene afforded the *N*-phenylfullerenopyrrolidine derivative **A-3PV** in 28% yield. Thanks to the presence of the three dodecyloxy substituents, compound **A-3PV** is well soluble in common organic solvents such as CH_2Cl_2, $CHCl_3$, THF, or toluene, and complete spectroscopic characterization was easily achieved. In the ^{1}H-NMR spectrum of **A-3PV** recorded in $CDCl_3$, all the anticipated signals are observed. In addition to the resonances arising from the 3PV moiety and the phenyl ring, a singlet and an AB quartet are seen at δ 6.09 and 5.32 ppm, respectively, corresponding to the signals of the protons of the pyrrolidine ring in full agreement with the C_1 symmetry of **A-3PV**. This lack of symmetry resulting from the presence of the stereogenic C atom in the pyrrolidine ring is also evidenced by the signal dispersion observed in the ^{13}C-NMR spectrum of **A-3PV**. The structure of **A-3PV** is confirmed by FAB-mass spectrometry with the molecular ion peak at m/z = 1672.8 ($[M + H]^+$, calculated for $C_{126}H_{98}NO_3$: 1672.74).

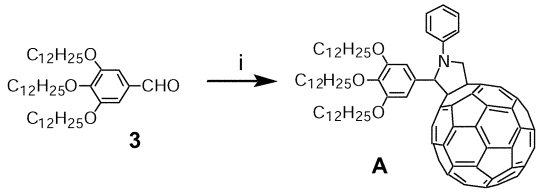

Scheme 2 *Reagents and conditions*: (i) C_{60}, *N*-phenylglycine, toluene, reflux, 16 h (10%).

Model fullerenopyrrolidine **A** was obtained by treatment of C_{60} with benzaldehyde **3**[30] and *N*-phenylglycine in refluxing toluene (Scheme 2).

The preparation of **B-3PV** is depicted in Scheme 3. Hydrazone **4** was obtained in 93% yield by treatment of aldehyde **2** with *p*-nitrophenylhydrazine in refluxing ethanol in the presence of acetic acid. Reaction of **4** with *N*-chlorosuccinimide (NCS) and subsequent reaction of the resulting nitrilimine (nitrile imide) intermediate with C_{60} under microwave irradiation[31,32] afforded **B-3PV** in 57% yield. The ^{1}H- and ^{13}C-NMR spectra of **B-3PV** show all the expected signals and are in full agreement with its C_s symmetry. The structure of **B-3PV** is also confirmed by MALDI-MS which shows the expected molecular ion peak at m/z = 1717.6 ($[M]^+$, calculated for $C_{125}H_{93}N_3O_5$: 1717.13).

Model compound **B** was prepared from aldehyde **3** following the same two step procedure (Scheme 4). Reaction of **3** with *p*-nitrophenylhydrazine followed by treatment of the resulting **5** with NCS and subsequent reaction with C_{60} under microwave irradiation gave **B**.

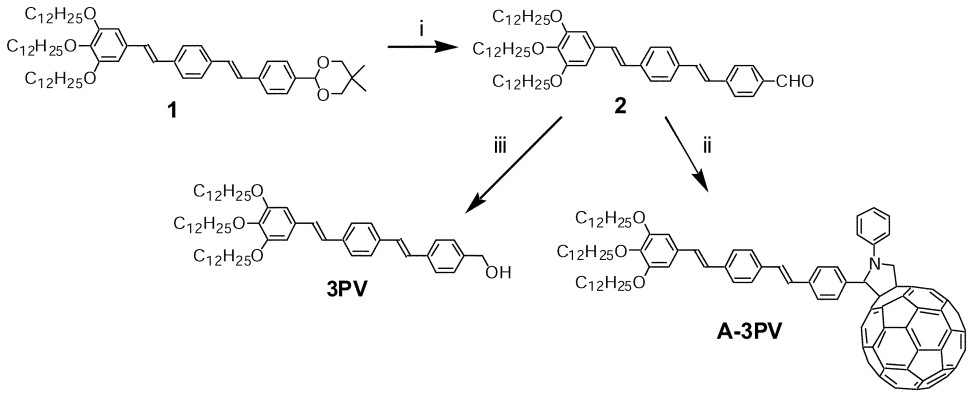

Scheme 1 *Reagents and conditions*: (i) CF_3CO_2H, H_2O, CH_2Cl_2, rt, 5 h (91%); (ii) C_{60}, *N*-phenylglycine, toluene, reflux, 7 days (28%); (iii) $LiAlH_4$, THF, 0 °C, 1 h (86%).

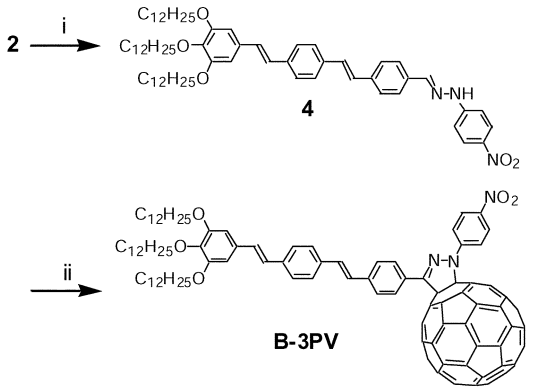

Scheme 3 *Reagents and conditions*: (i) *p*-nitrophenylhydrazine, AcOH, EtOH, reflux, 4.5 h (93%); (ii) NCS, pyridine, $CHCl_3$, 0 °C to rt, then C_{60}, Et_3N, toluene, microwave irradiation, 40 min (57%).

Electrochemistry

The results of cyclic voltammetry experiments are reported in Table 1. The reference compound **A** exhibits the typical fullerenopyrrolidine-type three reversible one-electron reduction steps, at about 100 mV more negative potentials than pristine C_{60}.[33,34] An irreversible one-electron oxidation step is also detected in **A** which is not observed in C_{60} and is attributed to the pyrrolidine nitrogen. Further oxidation also occurs, but the process is not well defined due to electrode inhibition. 3PV is oxidized at +0.62 V and reduced at a rather negative potential (−2.40 V), close to the electrolyte discharge. The three one-electron reduction processes in **A-3PV** are easily attributed to the fullerene unit, whereas the oxidation step occurs on the OPV branch and not on the fullerenopyrrolidine nitrogen.

The fullerenopyrazolines **B** and **B-3PV** exhibit three reversible one-electron reduction steps; the first two processes are attributable to the fullerene core. Fullerene derivatives usually possess higher reduction potentials than pristine C_{60} but, due to the inductive effect of the pyrazoline nitrogen directly attached to the carbon sphere, the potentials of pristine C_{60} are restored in **B** and **B-3PV**.[32,35] The third reduction at −1.65 V occurs on the nitrophenyl group as argued upon comparison with nitrobenzene, which is reduced at −1.61 V under these experimental conditions.[36] **B-3PV** is oxidized at +0.60 V, most likely on the OPV branch, whereas the first oxidation of **B** occurs at +0.80 V and can be localized on the pyrazoline sp^3 nitrogen.

In summary the electrochemical results suggest that in the dyads **A-3PV** and **B-3PV** the first oxidation step is located on the 3PV core and the two first reductions on the carbon cage. Interestingly, the two moieties also behave as independent redox centers in **B-3PV** where the OPV-type unit is conjugated with the pyrazoline ring.

Photophysical properties

Reference compounds 3PV and A. The electronic absorption spectrum of 3PV in CH_2Cl_2 solution is reported in Fig. 1. 3PV exhibits intense fluorescence both in fluid CH_2Cl_2 solution at 298 K (λ_{max} = 460 nm; Φ_{fl} = 0.77) and in a rigid matrix at 77 K (λ_{max} = 458 nm).[37] The luminescence lifetime at room temperature is monoexponential (1.3 ns), whereas at 77 K a biexponential decay is observed (τ_1 = 2.8 ns, τ_2 = 12.3 ns), probably as a consequence of the presence of different "frozen" rotameric forms in the solid matrix.[38] Accordingly, the fluorescence spectrum of 3PV at 77 K could be the result of a superimposition of two slightly shifted spectral profiles, and this would explain the lack of marked vibrational resolution (Fig. 1). In general, the spectroscopic properties of 3PV are in line with those of previously reported OPV's in organic solvents.[39]

Fullerenopyrrolidines are among the most widely investigated C_{60} derivatives.[29] The *N*-phenylfullerenopyrrolidine derivative **A** exhibits photophysical properties very similar to those of analogous *N*-methylfullerenopyrrolidines.[20,29] For the latter, ground and/or excited state electronic interactions between the fullerene carbon sphere and the nitrogen atom are not present as revealed, for instance, by fluorescence experiments in solvents of different polarity.[40] Therefore it is reasonable that, for **A**, conjugation of the nitrogen atom with a phenyl ring does not substantially affect the photophysical properties of the distant fullerene chromophore. The room temperature steady state electronic absorption spectrum and 77 K fluorescence band of **A** in CH_2Cl_2 are reported in Fig. 1. The singlet excited state lifetimes and fluorescence quantum yields of **A** in the same solvent are listed in Table 2. The

Table 1 Redox potential of the studied species observed in CH_2Cl_2 + 0.1 M Bu_4NPF_6 on a glassy carbon working electrode. All potentials are given *versus* ferrocene as standard

	Red_3/V^a	Red_2/V^a	Red_1/V^a	Ox_1/V^b	Ox_2/V^b
A	−2.00	−1.49	−1.10	+0.79 (E_p)	
A-3PV	−1.99	−1.44	−1.09	+0.60 (E_p)	+0.91 (E_p)
B	−1.65[c]	−1.36	−0.97	+0.80 (E_p)	
B-3PV	−1.64[c]	−1.34	−0.97	+0.60 (E_p)	
3PV			−2.40 (E_p)	+0.62 (E_p)	
C_{60}	−1.81	−1.37	−0.98		

[a]Reversible reduction: $E^o = (E_{pc} + E_{pa})/2$. [b]Peak potential at v = 0.1 Vs^{-1} for the irreversible oxidation step. [c]Reduction of the nitro group.

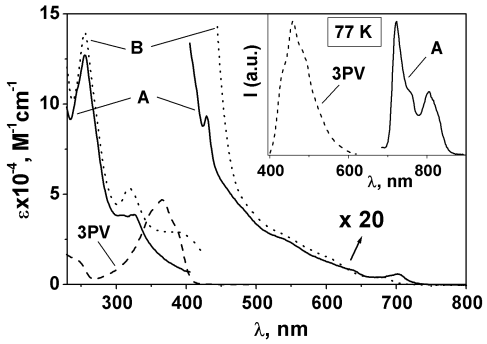

Fig. 1 Absorption spectra of **A** (——), **B** (···), and 3PV (– – –) in CH_2Cl_2. Inset: fluorescence spectra, corrected for the detector response, of **A** (——) and 3PV (– – –) in CH_2Cl_2 rigid matrix at 77 K.

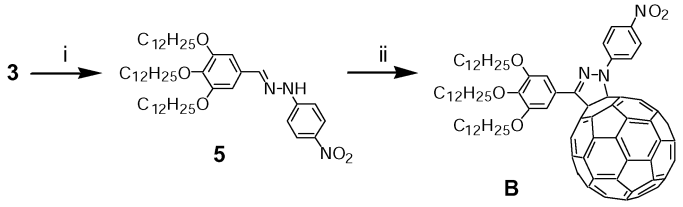

Scheme 4 *Reagents and conditions*: (i) *p*-nitrophenylhydrazine, AcOH, EtOH, reflux, 4 h (85%); (ii) NCS, pyridine, $CHCl_3$, 0 °C to rt, then C_{60}, Et_3N, toluene, microwave irradiation, 40 min (43%).

Table 2 Fullerene luminescence data in CH_2Cl_2, unless otherwise noted

	298 K			77 K	
	λ_{max}/nm[a]	$\Phi_{em} \times 10^4$	τ/ns[b]	λ_{max}/nm[a,c]	τ/ns[b]
A	714	5.5	1.0	722	1.5
A-3PV	710[d]	5.5[d]	1.1	718	1.6
B	706	< 0.1[e]	[f,g]	698	1.5
B + TFA[h]	690	1.3	0.76	[f]	[f]
B-3PV	708[d]	< 0.1[d]	[f]	700	[f]
	776[i]	3.5[i]	1.1[i]	704[i]	1.2[i]
B-3PV + TFA[h]	694[d]	0.16	0.75	[f]	[f]

[a]From emission spectra corrected for the photomultiplier response. [b]λ_{exc} = 337 nm, single photon counting spectrometer (see Experimental section). [c]Spectra obtained upon subtraction of the background signal due to the non-transparent matrix. [d]Excitation either on the OPV-type (365 nm) or fullerene-type (450 nm) moiety. [e]~0.35 in toluene. [f]Not measured due to signal weakness. [g]<0.5 ns in toluene. [h]30% (v/v) addition of trifluoroacetic acid (TFA). [i]In toluene solution.

triplet–triplet transient absorption spectrum of **A** in toluene is shown in Fig. 2; the triplet lifetime is 282 ns and 45 μs in air-equilibrated and air purged solution, respectively.

Fullerenopyrrolidine array A-3PV. The absorption spectrum of **A-3PV** in CH_2Cl_2 is reported in Fig. 3, along with the profile obtained by summing the spectra of its component units **A** and 3PV; some differences are evident. In OPV–C_{60} arrays investigated earlier, where the through bond and through space distances between the chromophores are identical to the present case, matching between the experimental and the model spectra was also not obtained.[21] This was attributed to different rotameric conformations of the OPV subunit unit when attached (or not) to the cumbersome C_{60}, rather than to strong ground state electronic interactions between the chromophores, that were not evident by electrochemistry.[21] Even in the present case the electrochemical results do not point to sizeable interactions; therefore a similar rationale to explain the differences found in the spectral profiles of Fig. 3 (top panel) can be proposed. Interestingly, when OPV and C_{60} subunits are located further apart, the absorption spectra of the arrays are identical to the sum of the component subunits.[20]

It is important to point out that the absorption features of the **A** and 3PV chromophores (Fig. 1) allow excitation selectivity in the dyad **A-3PV** to a large extent. In particular in the range 230–300 nm a nearly selective excitation of the C_{60} unit is possible, which becomes complete above 420 nm. On the other hand in the 350–390 nm range a good degree of selectivity for the OPV subunit is obtained; at 365 nm about 75% of the light is absorbed by such units.

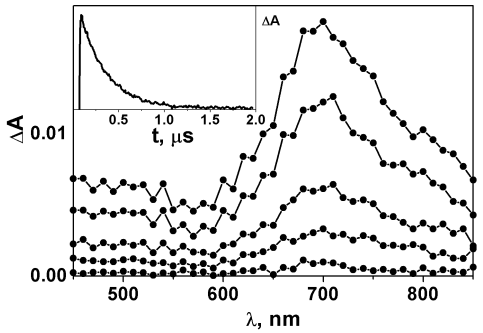

Fig. 2 Transient absorption spectrum of **A** at 298 K in toluene air-equilibrated solution upon laser excitation at 355 nm (energy = 3 mJ per pulse). The spectra were recorded at delays of 100, 200, 400, 600, and 1000 ns following excitation. The inset shows the time profile of ΔA (700 nm) from which the spectral kinetic data were obtained; the fitting is monoexponential and gives a lifetime of 282 ns.

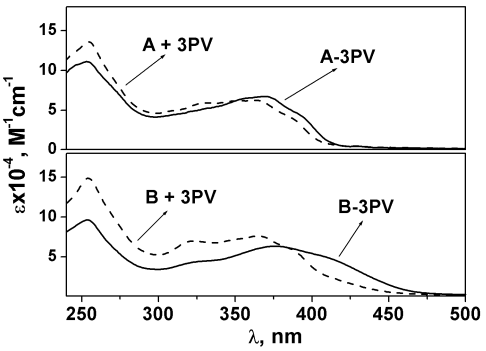

Fig. 3 Absorption spectra (——) of **A-3PV** (top) and **B-3PV** (bottom) in CH_2Cl_2 compared to those obtained (– – –) by summing the spectra of the corresponding reference compounds **A** + 3PV and **B** + 3PV.

Excitation of **A-3PV** at 365 nm in CH_2Cl_2 results in a 1000-fold decrease of fluorescence intensity relative to the reference compound 3PV under the same conditions. In parallel, sensitization of the fullerene lowest singlet excited state is observed since solutions of **A** and **A-3PV** displaying the same absorbance at 365 nm exhibit the same fullerene fluorescence intensity (Fig. 4). These results suggest that intramolecular singlet–singlet OPV → C_{60} energy transfer takes place.[20,21] This process is expected to be extremely fast (within about 1 ps following light excitation) considering the lifetime of unquenched 3PV (1.3 ns) and the dramatic decrease (about 1000 times) of the 3PV fluorescence. Model calculations on dipole–dipole Förster-type OPV → C_{60} energy transfer, performed as described earlier,[21] give an energy transfer rate constant (k_{en}) in the range 1×10^{12} to 1×10^{11} s^{-1} for donor–acceptor distances between 10 and 15 Å and a critical transfer radius R_c (*i.e.* the distance between the partners at which k_{en} equalizes the rate of the intrinsic deactivation of the donor) of 34 Å. Thus energy transfer is expected to be extremely fast as suggested earlier[21] and recently confirmed experimentally for OPV–C_{60} arrays.[41]

The occurrence of photoinduced energy or electron transfer processes in C_{60}-containing multicomponent arrays can be controlled by solvent polarity. Usually, energy transfer occurs in apolar media (*e.g.* toluene), whereas in polar solvents such as

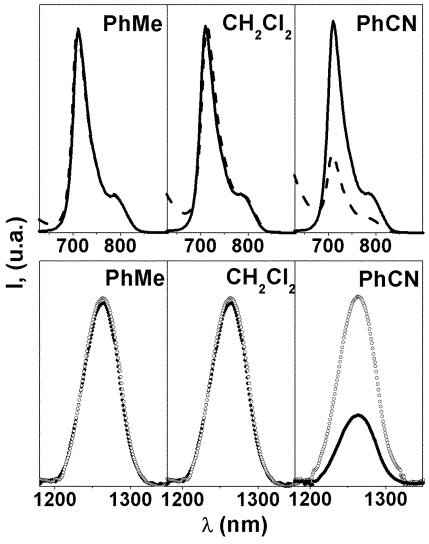

Fig. 4 Top: fluorescence spectra of **A** (——) and **A-3PV** (– – –) in toluene (PhMe), dichloromethane (CH_2Cl_2), and benzonitrile (PhCN); λ_{exc} = 365 nm, A = 0.200 for all samples. Bottom: sensitized singlet oxygen luminescence of **A** (○) and **A-3PV** (●) in the same solvents and under identical experimental conditions as above. The same spectral intensity ratios are obtained upon selective excitation of the fullerene moiety at 430 nm for both type of experiments.

benzonitrile electron transfer tends to prevail. These trends have been observed in a number of cases[42–44] including dyads containing organic conjugated oligomers.[22,26,45]

We have tested the luminescence behaviour of **A-3PV** in toluene (PhMe, static relative permittivity $\varepsilon = 2.4$) and benzonitrile (PhCN, $\varepsilon = 25.2$), and compared it to that in dichloromethane (CH_2Cl_2, $\varepsilon = 8.9$). Excitation of the 3PV moiety in PhMe and PhCN (and CH_2Cl_2, see above) leads to the same results: a 1000-fold decrease of the OPV fluorescence band intensity is observed both at 298 and 77 K. Importantly, upon excitation of the OPV moiety (365 nm), quantitative sensitization of the fullerene fluorescence is observed in PhMe, as in CH_2Cl_2; on the contrary, in PhCN, the recovery of this band is only 40% (Fig. 4). An identical trend in the relative intensities of the fullerene fluorescence bands, as a function of solvent polarity, is observed upon exclusive excitation of the fullerene moiety at $\lambda \geqslant 430$ nm. These results indicate that for **A-3PV** in benzonitrile, irrespective of the excitation wavelength, there is a 60% loss of fullerene singlet excited states, not observed in less polar media. This suggests that an additional deactivation pathway, quite competitive with the extensive intersystem crossing typical of C_{60} fullerenes,[46] is made available.

In order to get further insight into the photophysical processes following light excitation of **A-3PV**, the yield of formation of the lowest triplet excited state in the three solvents was measured. This was accomplished by taking advantage of the singlet oxygen sensitization process brought about by the lowest triplet state of fullerenes according to the following reaction scheme:[46,47]

$$C_{60} \xrightarrow{h\nu} {}^1C_{60}{}^* \xrightarrow{isc} {}^3C_{60}{}^* \xrightarrow{O_2} C_{60} + {}^1O_2{}^* \qquad (1)$$

where isc denotes intersystem crossing, and $^1O_2$* stands for $O_2(^1\Delta_g)$, commonly named "singlet oxygen". The excited $^1O_2$* state deactivates to the ground state giving rise to a characteristic IR emission band centred at $\lambda = 1268$ nm.[48] The quantum yield of singlet oxygen sensitization (Φ_Δ) and of fullerene triplet formation (Φ_T) are found to be identical for C_{60}, for its closed cage[49] or open cage[50] derivatives as well as for higher fullerenes like C_{70}[51] and C_{76}.[52] Therefore the determination of Φ_Δ (derived by recording the sensitized IR emission of $^1O_2$*) can be taken as an indirect evaluation of Φ_T for all fullerenes.[53] In Fig. 4 (bottom panel) are reported the sensitized singlet oxygen luminescence bands of **A-3PV** in the three solvents, with **A** used as internal reference in all cases. The relative $^1O_2$* luminescence intensity ratios (**A** : **A-3PV**) are identical by exciting both at 365 nm (OPV moiety) and at 430 nm (C_{60} subunit).

The spectra of Fig. 4 show that the relative amount of singlet that is formed (monitored by C_{60} fluorescence) is identical to that of triplet (monitored by sensitized $^1O_2$ luminescence) in any solvent. The singlet (Table 2) and triplet (Table 3) lifetimes of **A** and **A-3PV** are identical both in CH_2Cl_2 and in PhMe. In PhCN, instead, the singlet lifetime is reduced from 2.4 ns (**A**) to 1.1 ns (**A-3PV**), whereas the triplet lifetime is unchanged for the two compounds both in aerated and in deaerated solution (Table 3).

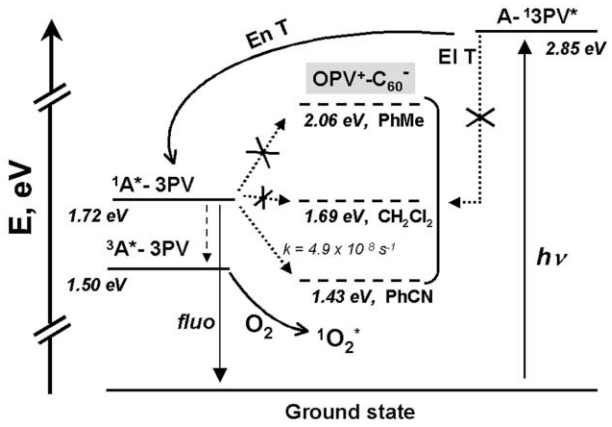

Fig. 5 Energy-level diagram describing excited state intercomponent processes following light excitation of the OPV subunit in **A-3PV**. Charge separated states are indicated as dashed lines, whereas full lines represent localized singlet and triplet electronic excited levels. EnT and EIT stand for energy-transfer and electron-transfer, respectively. For details on how the energy of the charge-separated and electronic excited states were estimated, see text.

The above experimental data can be rationalized with the aid of the diagram shown in Fig. 5. The energies of the lowest 3PV (A-^{1}3PV*) and fullerene (^{1}A*-3PV) singlet excited states have been estimated from the highest energy feature of the 77 K fluorescence spectra. A value of 1.50 eV for ^{3}A*-3PV is derived from the phosphorescence spectra of similar fullerenopyrrolidines.[54] The energy of the charge separated state in dichloromethane is obtained from the first oxidation and reduction potentials in this solvent (Table 1). The energy of the charge separated states in toluene and benzonitrile, for which electrochemical data are not available, are estimated by using the Weller equation:[55]

$$\Delta G_{CS} = q(E_{ox}(D) - E_{red}(A)) - E_{00} - \frac{q^2}{4\pi\varepsilon_0\varepsilon_s R_{DA}} - \frac{q^2}{8\pi\varepsilon_0}\left(\frac{1}{r^+} + \frac{1}{r^-}\right)\left(\frac{1}{\varepsilon_r} - \frac{1}{\varepsilon_s}\right) \qquad (2)$$

where q is elementary charge, E_{ox}(D) and E_{red}(A), are the oxidation and reduction potentials of the donor and the acceptor in the solvent with relative permittivity ε_r for which electrochemical data are available; ε_0 is the vacuum permittivity; E_{00} is the spectroscopic energy of the excited state from which the charge separation is promoted; R_{DA} is the center-to-center distance of the positive and negative charges in the charge-separated state; r^+ and r^- are the radii of the oxidized and reduced species; ε_s is the relative permittivity of the studied solvent. For our calculations we employed $r^- = 5.6$ Å[56] and $r^+ = 4.6$ Å (roughly estimated from the van der Waals volume of 3PV).[22] The center-to-center R_{DA} distance was estimated to be 12.5 Å from molecular modelling; the redox potentials are in Table 1; finally we used $E_{00} = 1.72$ eV corresponding to the energy of the lowest fullerene singlet excited state.

In toluene the pattern of photoinduced processes is straightforward and identical to that in dichloromethane.

Table 3 Relative intensities of sensitized singlet oxygen luminescence and triplet lifetimes obtained by transient absorption spectroscopy

	PhMe			CH_2Cl_2			PhCN		
	I_{Rel}	τ_{aer}/ns[a]	τ_{dea}/μs[b]	I_{Rel}	τ_{aer}/ns[a]	τ_{dea}/μs[b]	I_{Rel}	τ_{aer}/ns[a]	τ_{dea}/μs[b]
A	100	282	45	100	577	28	100	408	36
A-3PV	100	288	45	100	541	29	40	403	35
B	<10	[c]	[c]	<10	[c]	[c]	<10	[c]	[c]
B-3PV	100	307	44	<10	[c]	[c]	<10	[c]	[c]

[a]Air-equilibrated solution. [b]Air-free solutions. [c]The signals are too weak to obtain reliable results.

The quenching of the OPV fluorescence, followed by sensitization of the fullerene lowest singlet and triplet states, suggests the occurrence of efficient intramolecular OPV $\rightarrow C_{60}$ energy transfer followed by fullerene intersystem crossing. In PhMe electron transfer from ^{1}A*-3PV is not observed since it would be endergonic ($\Delta G_{CS} = 0.34$ eV). Importantly, such a process would be slightly exergonic in CH_2Cl_2 ($\Delta G_{CS} = -0.03$ eV), but it is disfavoured by a sizeable activation energy barrier (see below).

In PhCN, the fullerene singlet is quenched with a rate constant $k = 4.9 \times 10^8$ s^{-1}, as derived from luminescence lifetimes measurements. This process is ascribable to exergonic electron transfer ($\Delta G_{CS} = -0.29$ eV), see Fig. 5. The identical relative yields (compared to the reference compound **A**) of singlet and triplet formation and the unquenched triplet lifetimes show that electron transfer from the triplet state does not occur in this solvent. This implies that the observed triplet states are generated *via* intersystem crossing from the upper singlet level (Fig. 5, dashed arrow).

Competition between energy and electron transfer. In the investigated solvents the experimental results do not suggest the occurrence of electron transfer from the lowest singlet excited state of the 3PV moiety, though thermodynamically allowed (Fig. 5). According to the Marcus theory the maximum rate for charge separation is obtained for $\Delta G_{CS} = -\lambda$,[17] where λ is the reorganization energy and is the result of two contributions:

$$\lambda = \lambda_i + \lambda_e \quad (3)$$

where λ_i and λ_e are the internal (nuclear rearrangements) and external (of solvent origin) reorganization energies. For C_{60} dyads λ_i is 0.3 eV,[8,22] whereas λ_e can be estimated from the following equation:[56,57]

$$\lambda_e = \frac{q^2}{4\pi\varepsilon_0}\left(\frac{1}{2r^+} + \frac{1}{2r^-} - \frac{1}{R_{DA}}\right)\left(\frac{1}{n^2} - \frac{1}{\varepsilon_s}\right) \quad (4)$$

where n is the solvent refractive index. λ_e values of 0.05, 0.65, and 0.66 are calculated for PhMe, CH_2Cl_2 and PhCN, respectively. Within the Marcus approach it is then possible to calculate the energy of the activation barrier for charge separation according to eqn. (5):[17]

$$\Delta G^{\#}_{CS} = \frac{(\Delta G_{CS} + \lambda)^2}{4\lambda} \quad (5)$$

The data calculated from eqn. (2)–(5) and collected in Table 4 help to rationalize the trend of photoinduced processes displayed in Fig. 5. From these data the electron transfer from A-^{1}3PV* is concluded to be in the Marcus inverted region ($\Delta G_{CS} < -\lambda$)[17] in all solvents and this disfavours successful competition towards the ultrafast (subpicosecond)[21,41] singlet–singlet energy transfer. As for photoinduced processes arising from the lowest fullerene singlet ^{1}A*-3PV, it is seen (Table 4) that the activation energy barrier in CH_2Cl_2 is too high (0.22 eV) to allow the occurrence of charge separation, for which $\Delta G_{CS} = -0.03$ eV; this explains the lack of quenching processes in this solvent. In PhCN the charge separation process is located in the normal region of the Marcus parabola ($\Delta G_{CS} > -\lambda$)[17] and the reaction exergonicity is higher than the activation barrier. This allows sizeable competition with fullerene intrinsic deactivation, unlike the unfavourable cases of CH_2Cl_2 and PhMe. Attempts to directly detect the charge separated state *via* picosecond transient absorption spectroscopy in PhCN were unsuccessful since **A-3PV** decomposes under long-term high energy laser irradiation. In particular, UV–Vis ground state absorption spectra obtained after these experiments show a dramatic decrease of the OPV-type band centred at 365 nm. However, similar OPV–C_{60} dyads exhibit intramolecular charge separated states living about 50 ps in *o*-dichlorobenzene solution.[41]

Eqn. (6) describes the dependence of the rate for charge separation (k_{CS}) on the reorganization energy λ, the electron coupling between donor and acceptor V, and the activation energy $\Delta G^{\#}_{CS}$, in the so-called non-adiabatic regime:[56]

$$k_{CS} = \frac{2\pi^{3/2}}{h\sqrt{\lambda k_B T}} V^2 \exp\left[-\frac{\Delta G^{\#}_{CS}}{k_B T}\right] \quad (6)$$

Using the experimental k_{CS} in benzonitrile (4.9×10^8 s^{-1}), we can estimate a value of 26 cm^{-1} for V, when electron transfer is promoted from the lowest fullerene singlet excited state. Such a weak donor–acceptor coupling[41] is consistent with the electrochemical results and can support the interpretation of the ground state absorption spectrum (Fig. 3, top panel).

Fullerenopyrazoline B. The absorption spectrum of **B** in CH_2Cl_2 is reported in Fig. 1. An intense shoulder extending up to 500 nm is recorded, not present in the fullerenopyrrolidine **A**; a very weak band at about 680 nm ($\varepsilon \approx 200$ M^{-1} cm^{-1}) is attributable to the $S_0 \rightarrow S_1$ transition.

B exhibits a faint fluorescence band in CH_2Cl_2 at room temperature ($\lambda_{max} = 706$ nm), and the emission quantum yield is about two orders of magnitude lower than that of **A** (Table 2). The fluorescence intensity is dependent on solvent polarity; the lower the polarity the stronger the emission (Fig. 6). Fluorescence enhancing is obtained upon addition of trifluoroacetic acid (TFA) in CH_2Cl_2. At about 30% addition of TFA (v/v) an intensity plateau is reached (Fig. 6). The luminescence signal reverts to its initial intensity after extraction of

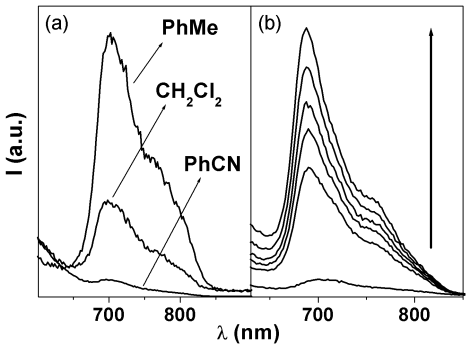

Fig. 6 (a) Fluorescence spectra of **B** in various solvents, under the same experimental conditions; $\lambda_{exc} = 430$ nm, $A = 0.400$. (b) Fluorescence spectrum of **B** in CH_2Cl_2 upon addition of increasing amount of acid up to 30% (v/v). $\lambda_{exc} = 424$ nm, isosbestic point.

Table 4 Reorganization energy (λ), free energy change (ΔG_{CS}), and activation barrier ($\Delta G^{\#}_{CS}$) for charge separation within **A-3PV** in toluene (PhMe), CH_2Cl_2 and benzonitrile (PhCN) upon excitation of the 3PV (A-^{1}3PV*) or fullerene (^{1}A*-3PV) lowest singlet states

		A-^{1}3PV*		^{1}A*-3PV	
	λ/eV	ΔG_{CS}/eV	$\Delta G^{\#}_{CS}$/eV	ΔG_{CS}/eV	$\Delta G^{\#}_{CS}$/eV
PhMe	0.35	−0.79	0.14	0.34	0.34
CH_2Cl_2	0.95	−1.16	0.01	−0.03	0.22
PhCN	0.96	−1.42	0.06	−0.29	0.12

the CH_2Cl_2–TFA solution with a saturated water solution of NaOH.

All these results suggest that the lowest fullerene singlet excited state is quenched by electron transfer from the lone pair of the pyrazoline sp^3 nitrogen, in analogy with similar substituted fullerenes.[8–13] Accordingly, we can describe the fullerenopyrazoline **B** as a redox dyad in which the electron donor and acceptor units are linked through an sp^3 carbon as a very simple spacer, as suggested by Sun *et al.* for aminofullerene derivatives.[9]

Fullerenopyrazoline array B-3PV. The absorption spectrum of **B-3PV** in CH_2Cl_2 is reported in Fig. 3 (bottom panel), along with the profile obtained by summing the spectra of the component units **B** and 3PV. Substantial differences are evident, definitely more pronounced than those found in the analogous comparison made for **A-3PV** (Fig. 3, top panel). This can be ascribed to the extended conjugation of the 3PV moiety in **B-3PV** as a result of the presence of an additional double bond; accordingly the absorption of the OPV subunit is found to be red-shifted.

Similarly to **B** a very weak fullerene-type fluorescence band is detected in CH_2Cl_2 for **B-3PV** ($\lambda_{exc} \geqslant 430$ nm), therefore, the same pyrazoline $\rightarrow C_{60}$ electron transfer quenching process must be active in the multicomponent array. Although in **B-3PV** the OPV moiety is easier to oxidize than the pyrazoline subunit (Table 1), prompt photoinduced electron transfer from the heteroaromatic ring is observed. This can be related to its closer vicinity to the electron accepting C_{60} moiety.

Excitation of **B-3PV** in CH_2Cl_2 at 365 nm, where a substantial part of the light is absorbed by the 3PV chromophore (Figs. 1 and 3), results in a 1000-fold decrease of fluorescence intensity relative to the reference compound 3PV under the same conditions. Although sensitization of the dramatically quenched fullerene fluorescence cannot be used as a probe, this quenching is attributed to singlet–singlet OPV $\rightarrow C_{60}$ energy transfer. For **B-3PV**, we have calculated that Förster-type singlet–singlet energy transfer can be as much as twice faster than for **A-3PV** (see above);[21] on the other hand electron transfer from B-^{1}3PV* is deeper in the inverted region ($\Delta G_{CS} = -1.28$ eV) than in the case of the fullerenopyrrolidine dyad ($\Delta G_{CS} = -1.16$ eV), assuming the same λ value (0.95 eV, eqn. (4)) for both arrays. This suggests that electron transfer is most likely not able to compete with energy transfer in **B-3PV**, in analogy with **A-3PV**. Unfortunately, also for such an array, direct detection of the charge separated state is prevented due to sample decomposition under prolonged laser irradiation.

Solvent and temperature dependence of the fullerene fluorescence. The addition of the same amount of acid to solutions of **B** and **B-3PV** in CH_2Cl_2, causes a much lower recovery of fullerene fluorescence for the latter compound (Table 2); this suggests differences in the electron transfer quenching process from the pyrazoline unit. We thus investigated in detail the dependence of such emission bands on solvent polarity and temperature, two factors that also affect electron-transfer processes. In Table 5 is reported the presence or the lack (ON/OFF) of the C_{60}-type fluorescence band in PhMe, CH_2Cl_2, and PhCN at 298 and 77 K; some indication of the emission relative intensities are specified in the footnotes. The data for **A** and **A-3PV** are also listed.

For the latter dyad the data of Table 5 provide further support for extensive electron transfer (about 60% yield, see above) in PhCN at 298 K. In fact the C_{60}-type fluorescence intensities of optically matched solution of **A** and **A-3PV** are identical at 77 K, unlike at 298 K. The lack of solvent repolarization in the rigid matrix destabilizes the A^--$3PV^+$ charge separated state to such an extent that electron transfer is no longer possible, differently from the behaviour at room temperature (Fig. 5).

Table 5 Occurrence of fullerene fluorescence as a function of temperature and solvent

	298 K			77 K		
	PhMe	CH_2Cl_2	PhCN	PhMe	CH_2Cl_2	PhCN
A	ON	ON	ON	ON	ON	ON
A-3PV	ON	ON	ON[a]	ON	ON	ON
B	OFF[b]	OFF[b]	OFF	ON	ON	OFF
B-3PV	ON	OFF[b]	OFF	ON	ON	OFF

[a]Reduced by 60% relative to **A**. [b]Some weak luminescence signal is detected, that displays solvent dependence (Fig. 6). Anyway here we labeled it as OFF, in a relative comparison with **B-3PV** in TOL, for which the "genuine" unquenched emission of the fullerenopyrazoline chromophore is observable.

B exhibits faint emission in PhMe and CH_2Cl_2 (Fig. 6, $\Phi_{fluo} < 10^{-5}$). Nonetheless, recovery of fluorescence intensity is achieved at 77 K, and "regular" fullerene singlet lifetimes of 1.2–1.5 ns are measured; this further substantiates the electron transfer quenching mechanism at 298 K, previously discussed. In the highly polar solvent PhCN electron transfer is not prevented even in the rigid medium since the fluorescence is OFF also at 77 K; in this solvent an identical behaviour is found for **B-3PV**.

The trend of **B-3PV** fullerene fluorescence as a function of solvent, temperature, and acid concentration is quite intriguing. In particular we note the following differences, relative to **B**: (i) a strong band in PhMe at 298 K, (Fig. 7, Tables 2 and 5); (ii) less pronounced intensity recovery upon addition of acid (about ten times less, Table 2).

These findings suggest that the electron donor unit of **B** (the sp^3 nitrogen lone pair) is not comparably effective in **B-3PV**. We tentatively attribute this surprising behaviour to delocalization of such electronic pair over the conjugated OPV–pyrazoline system in **B-3PV**, which implies weakening of its reducing (and basic) character. This process is able to prevent pyrazoline $\rightarrow C_{60}$ electron transfer in apolar PhMe at 298 K, but not OPV $\rightarrow C_{60}$ energy transfer.

Control over photoinduced processes in B-3PV. It has been demonstrated that in CH_2Cl_2 solution photoinduced energy transfer occurs in **A-3PV**, whereas electron transfer is evidenced in **B**. **B-3PV** can be considered a more sophisticated hybrid where both an OPV and a pyrazoline moieties are coupled with the carbon sphere subunit. Electrochemical results suggest a certain degree of electronic insulation between the OPV fragment and the rest of the molecule but, on the other hand, the photophysical results (see absorption spectra and fluorescence in toluene) would not lead to the same conclusion. This could raise debate on whether or not **B-3PV** can be strictly defined as a molecular OPV–pyrazoline–fullerene triad; this is a questionable matter and we prefer to stick to experimental facts. In CH_2Cl_2 quenching of *both* the OPV *and* of the

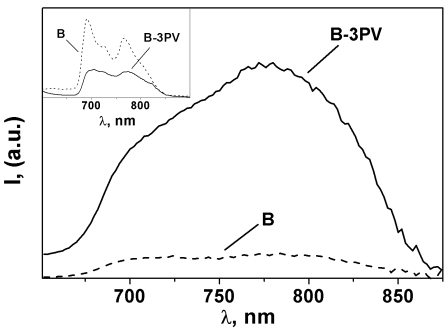

Fig. 7 Corrected fluorescence spectra of **B-3PV** (——) and **B** (– – –) in toluene at 298 and (inset) 77 K. $\lambda_{exc} = 430$ nm, $A = 0.400$.

Table 6 Summary of the photovoltaic characteristics for the devices prepared from **A-3PV** and **B-3PV**

Compound	V_{OC}/V	I_{SC}/A cm^{-2}	FF[a]	T^b (%)	S_{400}/A W^{-1}	$\eta_e{}^a{}_{400}$ (%)
A-3PV	0.38	3.4×10^{-7}	0.29	31	3.3×10^{-4}	3.8×10^{-3}
B-3PV	0.39	1.3×10^{-7}	0.26	3	1.3×10^{-4}	1.3×10^{-3}

[a]The calculation of the overall energy conversion efficiency η_e, has been done using the equation $\eta_e = \frac{V_{OC} I_{SC} FF}{P_{INC}}$ where V_{OC}, I_{SC}, FF and P_{INC} are the open circuit potential, short circuit current, filling factor and incident light power, respectively. The filling factor is given by $FF = \frac{V_{MAX} I_{MAX}}{V_{OC} I_{SC}}$ where V_{MAX} and I_{MAX} are voltage and current respectively, at the point of maximum power output. Standard intensity of light was 1 mW cm^{-2}. [b]T = transmission (corrected on glass, ITO and PEDOT-PSS).

fullerene fluorescence occur and this can be attributed to, respectively, (OPV → C_{60}) energy and (pyrazoline → C_{60}) electron transfer in analogy with the behaviour of **B** and **A-3PV**. The occurrence of distinct photoinduced processes can be confirmed by emission spectra in PhMe. In this solvent we observe quenching of the OPV fluorescence moiety accompanied by quantitative sensitization of the fullerene fluorescence. The occurrence of this latter band signals the suppression of photoinduced electron transfer in the apolar medium, while the OPV → C_{60} energy transfer process is kept active.

We can thus state that **B-3PV** is a multicomponent array featuring both an energy (3PV) and an electron transfer (pyrazoline) terminal, the fullerene moiety being able to act as energy or electron acceptor. Depending on the excitation wavelength one can control the nature of the photoinduced process. By exciting the OPV unit (*e.g.* at 365 nm, ~60% selectivity) an energy transfer to the C_{60} moiety, followed by pyrazoline → C_{60} electron transfer is obtained; by exciting the C_{60} fragment ($\lambda > 500$ nm, 100% selectivity) only electron transfer is triggered. Also chemical input (protons) and temperature (in CH_2Cl_2, Table 5) can affect the latter process, with no effect on the OPV → C_{60} energy transfer process, as already pointed out.

Incorporation in photovoltaic cells. Compounds **A-3PV** and **B-3PV** have been tested as active materials in photovoltaic devices, and the results are summarized in Table 6. Each C_{60}–OPV conjugate has been sandwiched between poly(3,4-ethylenedioxythiophene)poly(styrenesulfonate) (PEDOT-PSS)-covered indium tin oxide (ITO) and aluminium electrodes. The organic layers were prepared by spin coating from chloroform solutions and observations of the surface morphology by atomic force microscopy (AFM) in tapping mode revealed the obtaining of continuous and uniform films for all the compounds.

The current–voltage (*I–V*) curves of both devices have been recorded in the dark and under illumination and are depicted in Fig. 8. In the dark, the current is found to be higher by at least two orders of magnitude for the ITO/PEDOT-PSS/**A-3PV**/Al device when compared to the ITO/PEDOT-PSS/**B-3PV**/Al one. The latter observation is likely due to better charge transport properties of the thin films prepared from compound **A-3PV**. In the case of **B-3PV**, the lower conductivity may be ascribed to the presence of the pyrazoline N atom which is able to act as a trap due to its electron donating ability as evidenced by the electrochemical and photophysical studies.

Under illumination both devices show a clear photovoltaic behaviour although the rectifying ratio is not significantly large. The cells prepared from **A-3PV** display better overall performance characteristics although, by comparing their respective transmittance values, it is obvious that **B-3PV** exhibits enhanced absorption ability for the examined spectral region (Fig. 9). The sensitivity spectrum of both devices also follows their respective absorption spectrum as depicted in Fig. 9.

The monochromatic power conversion efficiency of the devices prepared from **A-3PV** is rather poor due to the low contribution of photoinduced electron transfer from the OPV moiety to the fullerene subunit. Most likely energy transfer is the main deactivation pathway also in the solid state, in line with the solution behaviour. This is in good agreement with previous studies on related systems.[21] Surprisingly, the performances of the devices obtained with **B-3PV** are not improved even if efficient electron transfer has been evidenced for this compound. Actually, it seems that the charge separation involving the fullerene moiety and the pyrazoline N atom is not able to contribute to the photocurrent production since it does not involve the hole conducting moiety (the 3PV unit). In other words, only the photoinduced electron transfer from the OPV unit to the fullerene moiety is efficient for the photovoltaic effect. Since the latter is a minor deactivation pathway, only a small part of the absorbed light is able to contribute effectively to the photocurrent.

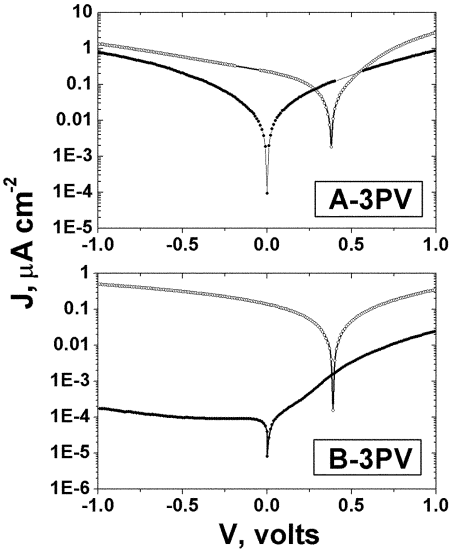

Fig. 8 Current–voltage (*I–V*) characteristics in the dark (●) and under illumination (○) for ITO/PEDOT-PSS/**A-3PV**/Al (top) and ITO/PEDOT-PSS/**B-3PV**/Al (bottom).

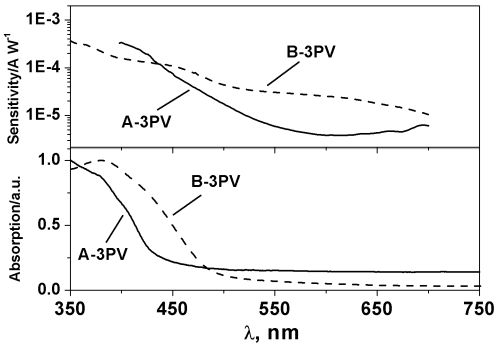

Fig. 9 Absorbance (bottom) and sensitivity (top) as a function of the illumination wavelength for the devices: ITO/PEDOT-PSS/**A-3PV**/Al (——); ITO/PEDOT-PSS/**B-3PV**/Al: (– – –).

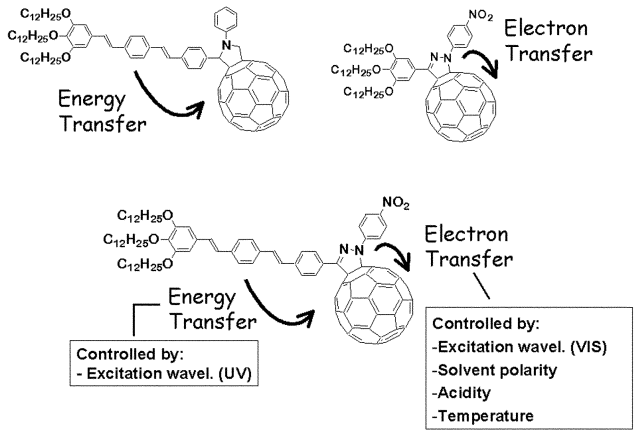

Fig. 10 Schematic representation summarizing the photoinduced processes occurring in **A-3PV**, **B**, and **B-3PV** in CH_2Cl_2 solution.

Conclusions

A-3PV and **B-3PV** are new multicomponent arrays where an OPV unit (3PV) has been linked to a fullerenopyrrolidine (**A**) or a fullerenopyrazoline (**B**) moiety. The photophysical properties of **A**, **B**, **A-3PV**, and **B-3PV** have been studied in three different solvents of increasing polarity, namely toluene, dichloromethane, and benzonitrile as well as at 298 and 77 K. Pyrazoline $\rightarrow C_{60}$ photoinduced electron transfer is observed at room temperature in **B** in all solvents and can be blocked by addition of acid or by passing to a rigid matrix at 77 K (PhMe and CH_2Cl_2 only). In **A-3PV** OPV $\rightarrow C_{60}$ energy transfer is evidenced in all solvents, followed by charge separation in PhCN to a significant extent.

B-3PV is arranged in such a way that the C_{60} unit can act either as energy (for OPV) or electron (for pyrazoline) acceptor, following light excitation. Excitation of the OPV moiety or of the fullerene chromophore triggers distinct photoprocesses. Further, besides the choice of excitation wavelength, the control over electron transfer is achieved by varying several (even combined) parameters, *i.e.* solvent polarity, acidity, and temperature. A schematic picture summarizing all these features in CH_2Cl_2 solution is depicted in Fig. 10.

Many cases of dyads made of a C_{60} unit and a conjugated oligomer have been reported so far,[19–22,24–27,45,58] and also cases of C_{60} coupled with an amine type donor have been described.[8–13] The integration of both features onto a C_{60} unit is reported here for the first time in **B-3PV**. This introduces a very interesting pattern of the photophysical properties in solution as shown schematically in Fig. 10, that make **B-3PV** a fullerene-based molecular switch, the switchable parameters being photoinduced processes. The incorporation of **B-3PV** in photovoltaic devices results in a lower light to current efficiency than in **A-3PV**, since charge separation involving the fullerene moiety and the pyrazoline N atom is not able to contribute to the photocurrent and, instead, the pyrazoline unit can act as an electron trap. Nevertheless we believe that the design of multicomponent arrays like **B-3PV**, featuring an antenna unit (OPV) and a charge separation module (pyrazoline–C_{60}) is very appealing for the construction of devices for charge separation and light energy conversion. Future work will be aimed at designing and testing new systems in which exciton dissociation is more efficiently achieved.

Experimental

Synthetic procedures and full characterization of all new molecules are available as electronic supplementary information.†

Electrochemistry

The electrochemical experiments were carried out at 20 ± 2 °C in CH_2Cl_2 containing 0.1 M Bu_4NPF_6 in a classical three electrode cell. The working electrode was a glassy carbon disk (3 mm in diameter) used motionless for cyclic voltammetry (sweep rates from 10 mV s^{-1} to 10 V s^{-1}). The auxiliary and the pseudo reference electrodes were platinum wires. All potentials are refereed to the ferrocenium/ferrocene (Fc^+/Fc) couple, which was used as internal standard. CH_2Cl_2 (Merck, spectroscopic grade) was dried over molecular sieves (4 Å) and used as such. Bu_4NPF_6 (Fluka, electrochemical grade) was used without further purification. The accessible potential window on the glassy carbon electrode in CH_2Cl_2 was +1.4 to −2.4 V *vs.* Fc^+/Fc. The cell was connected to a computerized multipurpose electrochemical device AUTOLAB (Eco Chemie BV, Utrecht, The Netherlands) controlled by the GPSE software running on a personal computer.

Photophysics

The photophysical investigations were carried out in CH_2Cl_2, and toluene (Carlo Erba, spectrofluorimetric grade), and in benzonitrile (Aldrich, HPLC grade). The samples were placed in fluorimetric 1 cm path cuvettes and, when necessary, purged from oxygen by at least four freeze–thaw–pump cycles. Absorption spectra were recorded with a Perkin-Elmer λ40 spectrophotometer. Uncorrected emission spectra were obtained with a Spex Fluorolog II spectrofluorimeter (continuous 150 W Xe lamp), equipped with a Hamamatsu R-928 photomultiplier tube. The corrected spectra were obtained *via* a calibration curve determined with a procedure described earlier.[5] Fluorescence quantum yields obtained from spectra on an energy scale (cm^{-1}) were measured with the method described by Demas and Crosby[59] using as standards air equilibrated solutions of quinine sulfate in 1 N H_2SO_4 (Φ = 0.546)[60] or $[Os(phen)_3]^{2+}$ in acetonitrile (Φ_{em} = 0.005).[61] To record the 77 K luminescence spectra, the samples were put in glass tubes (2 mm diameter) and inserted in a special quartz dewar, filled up with liquid nitrogen. When necessary, spectra of the glass matrix were recorded and then subtracted as background signal, in order to eliminate the contribution from light scattering.

The steady-state IR luminescence spectra were obtained with a constructed-in-house apparatus available at the Chemistry Department of the University of Bologna (Italy) and described in detail earlier.[5] A continuous 450 W Xenon lamp was used as light source, in order to be able to excite at any wavelength in the range 300–600 nm. The determination of the relative yields of singlet oxygen sensitization, according to Darmanyan and Foote,[62] was obtained by monitoring the singlet oxygen luminescence at 1268 nm and by comparing them with the suited C_{60} reference compound (**A** or **B**). Reference and dyad solutions were set at the same absorbance in the same solvent, making corrections due to these factors unnecessary.[62]

Emission lifetimes on the nanosecond time scale were determined with an IBH single photon counting spectrometer equipped with a thyratron gated nitrogen lamp working in the range 2–40 kHz (λ_{exc} = 337 nm, 0.5 ns time resolution); the detector was a red-sensitive (185–850 nm) Hamamatsu R-3237-01 photomultiplier tube.

Transient absorption spectra in the nanosecond–microsecond time domain were obtained by using the second or the third harmonic (532 or 355 nm) of a Nd : YAG laser (JK Lasers) with 20 ns pulse and 1–2 mJ of energy per pulse. Triplet lifetimes were obtained by averaging five different decays recorded around the maximum of the absorption peak (680–720 nm) The details on the flash-photolysis system are reported elsewhere.[63]

Experimental uncertainties are estimated to be ±8% for

lifetime determinations, $\pm 20\%$ for emission quantum yields, $\pm 5\%$ for relative emission intensities in the NIR, ± 1 nm and ± 5 nm for absorption and emission peaks respectively.

Preparation and characterization of the photovoltaic devices

Films of the active material were fabricated by spin-coating from solution onto ITO–covered glass substrates which were previously coated with a layer of poly (3,4-ethylenedioxythiophene)poly(styrenesulfonate) (PEDOT-PSS, BAYTRON P—Bayer AG). The aluminium (Al) top electrode, which typically had a thickness of about 100 nm, was vapour-deposited at pressures of about 3×10^{-7} torr onto the organic layer. All other fabrication and measurement steps were carried out under nitrogen atmosphere to minimise effects of water and oxygen.

The devices were illuminated from the ITO side (400 nm, 1 mW cm^{-2}) using an Oriel 60100 xenon lamp in series with a CVI Digikrom 120 monochromator, while the *I–V* curves were measured with a Keithley 236 source measure unit. In forward bias, the ITO electrode was wired as the anode. A standard calibrated silicon photodiode was used to record the action photovoltaic spectra. UV/Vis absorption spectra were recorded on a Perkin Elmer 900 spectrophotometer and a Digital Instruments Nanoscope IIIa atomic force microscope was used for the imaging of the films.

Acknowledgement

This work was supported by the CNR-CNRS project "Supramolecular Fullerene Systems as Materials for Solar Energy Conversion", ECODEV, French Ministry of Research, Dutch Science Foundation and Spanish DGI (Project BQU2001-1512). We thank Professor A. Juris (Department of Chemistry, University of Bologna) for allowing the use of the IR spectrofluorimeter and Dr Francesco Barigelletti for calculations on energy transfer rates. G. A. thanks MIUR (Progetto 5%), D.T. EU (Marie Curie Fellowship), and J.-F. E. DGA for their fellowships. We further thank L. Oswald and M. Minghetti for technical help and M. Schmitt for NMR measurements.

References

1 D. Gust, T. A. Moore and A. L. Moore, *Acc. Chem. Res.*, 2001, **34**, 40.
2 D. M. Guldi and M. Prato, *Acc. Chem. Res.*, 2000, **33**, 695.
3 N. Martin, L. Sanchez, B. Illescas and I. Perez, *Chem. Rev.*, 1998, **98**, 2527.
4 H. Imahori, M. E. El-Khouly, M. Fujitsuka, O. Ito, Y. Sakata and S. Fukuzumi, *J. Phys. Chem. A*, 2001, **105**, 325.
5 N. Armaroli, G. Marconi, L. Echegoyen, J. P. Bourgeois and F. Diederich, *Chem. Eur. J.*, 2000, **6**, 1629.
6 N. Martin, L. Sanchez, M. A. Herranz and D. M. Guldi, *J. Phys. Chem. A*, 2000, **104**, 4648.
7 N. Armaroli, F. Diederich, C. O. Dietrich-Buchecker, L. Flamigni, G. Marconi, J. F. Nierengarten and J. P. Sauvage, *Chem. Eur. J.*, 1998, **4**, 406.
8 R. M. Williams, J. M. Zwier and J. W. Verhoeven, *J. Am. Chem. Soc.*, 1995, **117**, 4093.
9 Y. P. Sun, B. Ma and C. E. Bunker, *J. Phys. Chem. A*, 1998, **102**, 7580.
10 K. G. Thomas, V. Biju, M. V. George, D. M. Guldi and P. V. Kamat, *J. Phys. Chem. A*, 1998, **102**, 5341.
11 G. E. Lawson, A. Kitaygorodskiy and Y. P. Sun, *J. Org. Chem.*, 1999, **64**, 5913.
12 S. Komamine, M. Fujitsuka, O. Ito, K. Moriwaki, T. Miyata and T. Ohno, *J. Phys. Chem. A*, 2000, **104**, 11497.
13 F. Langa, P. de la Cruz, E. Espildora, A. Gonzalez-Cortes, A. de la Hoz and V. Lopez-Arza, *J. Org. Chem.*, 2000, **65**, 8675.
14 D. M. Guldi, *Chem. Commun.*, 2000, 321.
15 H. Imahori, K. Hagiwara, T. Akiyama, M. Aoki, S. Taniguchi, T. Okada, M. Shirakawa and Y. Sakata, *Chem. Phys. Lett.*, 1996, **263**, 545.
16 H. Imahori and Y. Sakata, *Eur. J. Org. Chem.*, 1999, 2445.
17 R. A. Marcus and N. Sutin, *Biochim. Biophys. Acta*, 1985, **811**, 265.
18 L. C. Sun, L. Hammarstrom, B. Akermark and S. Styring, *Chem. Soc. Rev.*, 2001, **30**, 36.
19 J. F. Nierengarten, J. F. Eckert, J. F. Nicoud, L. Ouali, V. Krasnikov and G. Hadziioannou, *Chem. Commun.*, 1999, 617.
20 N. Armaroli, F. Barigelletti, P. Ceroni, J. F. Eckert, J. F. Nicoud and J. F. Nierengarten, *Chem. Commun.*, 2000, 599.
21 J. F. Eckert, J. F. Nicoud, J. F. Nierengarten, S. G. Liu, L. Echegoyen, F. Barigelletti, N. Armaroli, L. Ouali, V. Krasnikov and G. Hadziioannou, *J. Am. Chem. Soc.*, 2000, **122**, 7467.
22 E. Peeters, P. A. van Hal, J. Knol, C. J. Brabec, N. S. Sariciftci, J. C. Hummelen and R. A. J. Janssen, *J. Phys. Chem. B*, 2000, **104**, 10174.
23 G. Accorsi, N. Armaroli, J. F. Eckert and J. F. Nierengarten, *Tetrahedron Lett.*, 2002, **43**, 65.
24 S. Knorr, A. Grupp, M. Mehring, G. Grube and F. Effenberger, *J. Chem. Phys.*, 1999, **110**, 3502.
25 T. Yamashiro, Y. Aso, T. Otsubo, H. Q. Tang, Y. Harima and K. Yamashita, *Chem. Lett.*, 1999, 443.
26 M. Fujitsuka, O. Ito, T. Yamashiro, Y. Aso and T. Otsubo, *J. Phys. Chem. A*, 2000, **104**, 4876.
27 P. A. van Hal, J. Knol, B. M. W. Langeveld-Voss, S. C. J. Meskers, J. C. Hummelen and R. A. J. Janssen, *J. Phys. Chem. A*, 2000, **104**, 5974.
28 J. F. Eckert, J. F. Nicoud, D. Guillon and J. F. Nierengarten, *Tetrahedron Lett.*, 2000, **41**, 6411.
29 M. Prato and M. Maggini, *Acc. Chem. Res.*, 1998, **31**, 519.
30 G. Zerban and H. Meier, *Z. Naturforsch., B: Chem. Sci.*, 1993, **48**, 171.
31 P. de la Cruz, A. Diaz-Ortiz, J. J. Garcia, M. J. Gomez-Escalonilla, A. de la Hoz and F. Langa, *Tetrahedron Lett.*, 1999, **40**, 1587.
32 F. Langa, P. de la Cruz, E. Espildora, A. de la Hoz, J. L. Bourdelande, L. Sanchez and N. Martin, *J. Org. Chem.*, 2001, **66**, 5033.
33 M. Maggini, A. Karlsson, G. Scorrano, G. Sandona, G. Farnia and M. Prato, *J. Chem. Soc., Chem. Commun.*, 1994, 589.
34 W. Kutner, K. Noworyta, G. R. Deviprasad and F. D'Souza, *J. Electrochem. Soc.*, 2000, **147**, 2647.
35 F. Langa, M. J. Gomez-Escalonilla, E. Diez-Barra, J. C. Garcia-Martinez, A. de la Hoz, J. Rodriguez-Lopez, A. Gonzalez-Cortes and V. Lopez-Arza, *Tetrahedron Lett.*, 2001, **42**, 3435.
36 R. E. Martin, U. Gubler, C. Boudon, C. Bosshard, J. P. Gisselbrecht, P. Gunter, M. Gross and F. Diederich, *Chem. Eur. J.*, 2000, **6**, 4400.
37 N. Armaroli, J. F. Eckert and J. F. Nierengarten, *Chem. Commun.*, 2000, 2105.
38 U. Mazzucato and F. Momicchioli, *Chem. Rev.*, 1991, **91**, 1679.
39 H. Meier, *Angew. Chem., Int. Ed. Engl.*, 1992, **31**, 1399.
40 B. Ma, C. E. Bunker, R. Guduru, X. F. Zhang and Y. P. Sun, *J. Phys. Chem. A*, 1997, **101**, 5626.
41 P. A. van Hal, R. A. J. Janssen, G. Lanzani, G. Cerullo, M. Zavelani-Rossi and S. De Silvestri, *Phys. Rev. B*, 2001, **6407**, 5206.
42 D. Kuciauskas, S. Lin, G. R. Seely, A. L. Moore, T. A. Moore, D. Gust, T. Drovetskaya, C. A. Reed and P. D. W. Boyd, *J. Phys. Chem.*, 1996, **100**, 15926.
43 T. D. M. Bell, T. A. Smith, K. P. Ghiggino, M. G. Ranasinghe, M. J. Shephard and M. N. Paddon-Row, *Chem. Phys. Lett.*, 1997, **268**, 223.
44 C. Luo, D. M. Guldi, H. Imahori, K. Tamaki and K. Sakata, *J. Am. Chem. Soc.*, 2000, **122**, 6535.
45 J. L. Segura, R. Gomez, N. Martin, C. P. Luo, A. Swartz and D. M. Guldi, *Chem. Commun.*, 2001, 707.
46 R. R. Hung and J. J. Grabowski, *J. Phys. Chem.*, 1991, **95**, 6073.
47 J. W. Arbogast, A. P. Darmanyan, C. S. Foote, Y. Rubin, F. N. Diederich, M. M. Alvarez, S. J. Anz and R. L. Whetten, *J. Phys. Chem.*, 1991, **95**, 11.
48 F. Wilkinson, W. P. Helman and A. B. Ross, *J. Phys. Chem. Ref. Data*, 1995, **24**, 663.
49 R. V. Bensasson, E. Bienvenue, C. Fabre, J. M. Janot, E. J. Land, S. Leach, V. Leboulaire, A. Rassat, S. Roux and P. Seta, *Chem. Eur. J.*, 1998, **4**, 270.
50 R. Stackow, G. Schick, T. Jarrosson, Y. Rubin and C. S. Foote, *J. Phys. Chem. B*, 2000, **104**, 7914.
51 R. V. Bensasson, M. Schwell, M. Fanti, N. K. Wachter, J. O. Lopez, J.-M. Janot, P. R. Birkett, E. J. Land, S. Leach, P. Seta, R. Taylor and F. Zerbetto, *ChemPhysChem.*, 2001, 109.

52 R. V. Bensasson, E. Bienvenue, J. M. Janot, E. J. Land, S. Leach and P. Seta, *Chem. Phys. Lett.*, 1998, **283**, 221.
53 R. V. Bensasson, M. N. Berberan-Santos, M. Brettreich, J. Frederiksen, H. Gottinger, A. Hirsch, E. J. Land, S. Leach, D. J. McGarvey, H. Schonberger and C. Schroder, *Phys. Chem. Chem. Phys.*, 2001, **3**, 4679.
54 D. M. Guldi and K. D. Asmus, *J. Phys. Chem. A*, 1997, **101**, 1472.
55 A. Weller, *Z. Phys. Chem. Neue Folge*, 1982, **133**, 93.
56 R. M. Williams, M. Koeberg, J. M. Lawson, Y. Z. An, Y. Rubin, M. N. Paddon-Row and J. W. Verhoeven, *J. Org. Chem.*, 1996, **61**, 5055.
57 J. Kroon, J. W. Verhoeven, M. N. Paddon-Row and A. M. Oliver, *Angew. Chem., Int. Ed. Engl.*, 1991, **30**, 1358.
58 J. L. Segura, R. Gomez, N. Martin, C. P. Luo and D. M. Guldi, *Chem. Commun.*, 2000, 701.
59 J. N. Demas and G. A. Crosby, *J. Phys. Chem.*, 1971, **75**, 991.
60 S. R. Meech and D. J. Philips, *J. Photochem.*, 1983, **23**, 193.
61 E. M. Kober, J. V. Caspar, R. S. Lumpkin and T. J. Meyer, *J. Phys. Chem.*, 1986, **90**, 3722.
62 A. P. Darmanyan and C. S. Foote, *J. Phys. Chem.*, 1993, **97**, 5032.
63 L. Flamigni, *J. Phys. Chem.*, 1992, **96**, 3331.